Radiation Physics and Chemistry 120 (2016) 38–43

Contents lists available at ScienceDirect

Radiation Physics and Chemistry

journal homepage: www.elsevier.com/locate/radphyschem

# Spontaneous emission of radiation by relativistic electrons in a gyro-klystron

G. Mishra *, Bramha Prakash, Geetanjali Sharma [1]

*Department of Physics, Devi Ahilya University (DAVV), Indore, Madhya Pradesh 452001, India*

## HIGHLIGHTS

- The paper presents a new scheme of gyro-klystron device and calculates spontaneous emission of radiation of electron in the gyro-klystron.
- The analysis is based on solution of Lienard Wiechert potential in far field limit and compares the results with an optical klystron undulator device.
- A practical device based on the analysis is suggested.

## ARTICLE INFO

*Article history:*
Received 22 July 2015
Received in revised form
24 October 2015
Accepted 27 November 2015
Available online 28 November 2015

*Keywords:*
Undulator
Optical klystron
Electron cyclotron maser

## ABSTRACT

In this paper, we study spontaneous emission of radiation by relativistic electrons in a gyro-klystron. The scheme consists of two solenoid sections separated by a dispersive section. In the dispersive section the electrons are made non resonant with the radiation. The dispersive section transforms a small change of the velocity into changes of the phases of the electrons.This leads to enhanced radiation as compared to a conventional gyrotron type device driven by cyclotron maser interaction. It is shown that the klystron modulated spectrum depends on the dispersive field strength, finite perpendicular velocity component and length of the solenoids but do not depend on the axial magnetic field strength. The analysis is further extended to include the combined effects of the undulator aided gyrotron klystron radiation.



## 1. Introduction

There exist interests in free electron lasers (FEL) (Margaritondo and Rebernick Ribic, 2011; McNeil and Thompson, 2010) and cyclotron resonance masers (Du and Liu, 2014; Bertolotti, 2015; Chu, 2004) as a tunable light source to produce high power coherent radiation over a wide wavelength range. In a FEL schematic, the relativistic electron beam travels through a wiggler/ undulator field and undergoes transverse oscillations. The device operates both in amplifier and oscillator mode either through co-propagating laser light or with mirror. On the other hand, in a electron cyclotron resonance maser, the relativistic electron beam with initial finite transverse velocity component travels in an axial magnetic field to emit coherent emission of radiation via cyclotron resonance maser interaction.A comparison of both the mechanisms have been discussed by many authors (Chu, 2004; Amnon Fruchtman, 1988; Danly et al., 1992). The undulator is the key component of the FEL (Marie Emmanuelle Couprie, 2014) and has undergone several important improvements and modifications over the past few decades and find increased applications in free electron lasers and inverse free electron lasers. Studies on two frequency undulator (Iracane and Bamas, 1991; Ciocci et al., 1993), bi-harmonic undulator (Dattoli et al., 2002; Dattoli et al., 2006; Kong et al., 2000; Gupta and Mishra, 2006), variable period undulator (Vinokurov et al., 2011), RF undulator (Kuzikov et al., 2013) have been reported for its novel properties for FEL and IFEL applications. In recent years there is increased interests in optical klystron undulator free electron laser (OKFEL) for enhanced laser gain (Jain and Mishra, 2014; Freund, 2013). The OKFEL uses two sections of undulator with a dispersive section in between. In the first section of the undulator i.e. modulator, the electron undergoes transverse oscillations and accelerations. The dispersive section is either a three or four section chicane where the electrons get modulation without resonance interaction. Without resonant interaction in the dispersive section, the small changes of the electron velocity leads to phase modulation and this leads to enhanced emission of radiation in the second section of the undulator called the radiator (Dattoli and Bucci, 2000; Dattoli et al., 1993; Dattoli and Bucci, 2000; Gehlot and Mishra, 2010; Elleaume, 1986; Kong, 1996). There are several studies on optical klystron

* Corresponding author.
*E-mail address:* gmishra_dauniv@yahoo.co.in (G. Mishra).
[1] Insertion Device Group, Soleil Synchrotron Facility, Paris, France.

http://dx.doi.org/10.1016/j.radphyschem.2015.11.024
0969-806X/

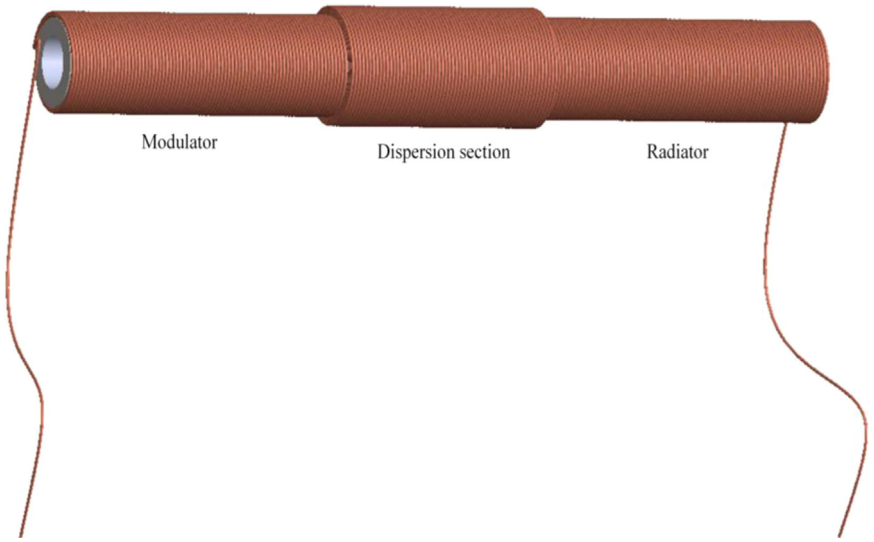


**Fig. 1.** Schematic of a proposed gyro-klystron.

undulator that explains the modeling of the dispersive section (Boscolo and Colson, 1985; Colson and Fredman, 1983; Gallardo and Pellegrini, 1990; Gallardo and Pellegrini, 1990; Thomas et al., 2002; Elleaume, 1983).

In this paper we consider the theory of optical klystron undulator radiation and propose a gyro-klystron device with two sections of solenoids producing the axial magnetic field are separated by a dispersive section. The schematic is similar to an optical klystron undulator where the two undulator sections are separated by a dispersive section. The two solenoid sections having equal lengths and equal number of turns are separated by a dispersive section. The electrons undergo cyclotron resonance oscillations in the modulator section i.e $\omega = s\Omega_c$, $\Omega_c$ is the relativistic cyclotron frequency. The dispersive section is considered as a section of the solenoid having more number of turns or a large current to have a large axial magnetic field. The large value of the axial magnetic field detunes the cyclotron resonance and allows the electrons to get phase modulation in response to a slow change in velocity. In Section 2, the Lienard-Wiechert potential is solved and an analytical expression is derived for the gyro-klystron radiation. The results are discussed in Section 3. The analysis describes the spike pattern of the gyro-klystron radiation (Figs. 2 and 3) and compared with the klystron undulator radiation. In an optical-klystron undulator the spikes depends on number of undulator parameter, undulator period and the undulator gap. In contrast, the spikes in the gyro-klystron depend on the finite perpendicular velocity component, length of the solenoid but do not depend on the solenoid magnetic field strength. In both the case the spikes vanish in the limit $D \to 0$ and gets closer with large value of the dispersive field strength. Finally a practical scheme is proposed for fabrication of the gyro-klystron with a discussion on undulator aided gyro klystron radiation.

## 2. Gyro-klystron radiation

The energy radiated per solid angle per unit frequency of a relativistic electron is evaluated from the Lienard–Wiechert potential (Jackson, 1962),

$$\frac{d^2I}{d\Omega d\omega} = \frac{e^2\omega^2}{4\pi^2 c}\left|\int_{-\infty}^{\infty}\left\{\hat{n}\times\left(\hat{n}\times\vec{\beta}\right)\right\}\exp\left[i\omega\left(t-\frac{\hat{n}\cdot\vec{r}}{c}\right)\right]dt\right|^2 \quad (1)$$

Where $e$ is the electron charge, $c$ is the velocity of the light in vacuum, $\omega$ is the radiation frequency, $\vec{\beta}$ is the electron normalized velocity, $\vec{r}$ is the electron trajectory and $\hat{n}$ is an observation unit vector. In Eq. (1) the integral is done in a region where the electron experiences an effective acceleration. The observation unit vector with components is written as, $\hat{n} = \psi\cos\phi,\ \psi\sin\phi,\ 1-\psi^2/2, \psi$ is the observation angle and $\phi$ is the azimuthal angle. The electron trajectories in an axial magnetic field can be determined from the Lorentz force equation and is given by

$$\begin{aligned}\beta_x &= \beta_\perp\cos(\Omega_c t)\\ \beta_y &= -\beta_\perp\sin(\Omega_c t)\\ \beta_z &= \beta^*,\ \beta^* = 1-\frac{1}{2\gamma^2}-\frac{\beta_\perp^2}{2}\end{aligned} \quad (2)$$

where $\Omega_c = \frac{eB_w}{\gamma m_0 c}$ is the relativistic cyclotron frequency of electron cyclotron motion and $\beta_x(0) = \beta_y(0) = \beta_\perp$ is the perpendicular initial velocity component. We consider two solenoid sections arranged in klystron configuration with a dispersive section '$D$' in between, where $D = L_d/L$ is the dimensionless length of the dispersive section, $L_d$ is the length of dispersive section and $L$ is the length of solenoid section. We assume that two solenoid sections have same length with equal number of turns. The schematic is illustrated in Fig. 1.The integral in Eq. (1) can be written as,

$$\int_{-\infty}^{\infty} dt\,(.....) = \int_0^T dt\,(.....) + \int_{T(1+D)}^{T(2+D)} dt\,(.....) \quad (3)$$

$T = N\lambda_u/\beta_z c$ is the flight time of the electron in one solenoid section. $\beta_z c$ is the average electron longitudinal velocity. We introduce Eq. (3) to redefine Eq. (1) as,

$$\frac{d^2I}{d\omega d\Omega} = \frac{e^2}{4\pi^2 c}\left|\omega\vec{T}\right|^2 \quad (4)$$

$$\text{with } \vec{T} = \int_0^T\left\{\hat{n}\times\left(\hat{n}\times\vec{\beta}\right)\right\}\exp\left[i\omega\left(t-\frac{\hat{n}\cdot\vec{r}}{c}\right)\right]dt + \int_{T(1+D)}^{T(2+D)}\left\{\hat{n}\times\left(\hat{n}\times\vec{\beta}\right)\right\}\exp\left[i\omega\left(t-\frac{\hat{n}\cdot\vec{r}}{c}\right)\right]dt \quad (5)$$

The finite components of the cross product appearing in Eq. (5) is evaluated to read as,